Structure
Article

Structure of BeF_3^--Modified Response Regulator PleD: Implications for Diguanylate Cyclase Activation, Catalysis, and Feedback Inhibition

Paul Wassmann,[1] Carmen Chan,[1,3] Ralf Paul,[2] Andreas Beck,[1] Heiko Heerklotz,[1,4] Urs Jenal,[2] and Tilman Schirmer[1,*]
[1] Core Program of Structural Biology and Biophysics
[2] Focal Area of Growth and Development
Biozentrum, University of Basel, Klingelbergstrasse 70, CH-4056 Basel, Switzerland
[3] Present address: Lonza Biopharmaceuticals, Lonza Ltd., CH-3930 Visp, Switzerland.
[4] Present address: Leslie Dan Faculty of Pharmacy, University of Toronto, 144 College Street, Toronto, Ontario M5S 3M2, Canada.
*Correspondence: tilman.schirmer@unibas.ch
DOI 10.1016/j.str.2007.06.016

SUMMARY

Cyclic di-guanosine monophosphate (c-di-GMP) is a ubiquitous bacterial second messenger involved in the regulation of cell surface-associated traits and persistence. We have determined the crystal structure of PleD from *Caulobacter crescentus*, a response regulator with a diguanylate cyclase (DGC) domain, in its activated form. The BeF_3^- modification of its receiver domain causes rearrangement with respect to an adaptor domain, which, in turn, promotes dimer formation, allowing for the efficient encounter of two symmetric catalytic domains. The substrate analog GTPαS and two putative cations are bound to the active sites in a manner similar to adenylate cyclases, suggesting an analogous two-metal catalytic mechanism. An allosteric c-di-GMP-binding mode that crosslinks DGC and an adaptor domain had been identified before. Here, a second mode is observed that crosslinks the DGC domains within a PleD dimer. Both modes cause noncompetitive product inhibition by domain immobilization.

INTRODUCTION

The central role of bis-(3′ → 5′)-cyclic di-guanosine monophosphate (c-di-GMP) as a signaling molecule has been realized only upon the recent recognition of the omnipresence of genes coding for diguanylate cyclase domains (DGC or GGDEF domains) in bacterial genomes. C-di-GMP regulates cell surface-associated traits and community behavior such as biofilm formation in most eubacteria (Jenal and Malone, 2006), and its relevance to the virulence of pathogenic bacteria has been demonstrated (Tischler and Camilli, 2004). In particular, the dinucleotide has been proposed to orchestrate the switch between acute and persistent phases of infection (Malone et al., 2007). C-di-GMP is synthesized out of two molecules of GTP and is degraded into the linear dinucleotide pGpG by the opposing activities of DGCs and c-di-GMP-specific phosphodiesterases. Both enzymes occur in combinations with various other, mostly sensory or regulatory, domains. It is believed that in this way environmental or internal stimuli can control the production of c-di-GMP, which, in turn, will affect downstream targets (Jenal and Malone, 2006). One of these c-di-GMP effector domains (PilZ) has recently been identified (Amikam and Galperin, 2006; Christen et al., 2007).

About 10% of the known DGCs are response regulators (RRs) as part of two-component systems (Jenal and Malone, 2006). RRs are activated by cognate histidine kinases that phosphorylate a conserved aspartate of the receiver domain (Rec) (Stock et al., 2000). Various Rec domains have been studied in great detail, and the structural changes upon activation have been described (for a review, see Robinson et al., 2000).

Due to the instability of the aspartyl phosphoanhydride, these studies have been performed with phosphoryl analogs. Notably, modification of CheY by beryllium fluoride (BeF_3^-) (Lee et al., 2001) resulted in structural changes fully equivalent to those obtained by phosphorylation (Birck et al., 1999; Lewis et al., 1999). Upon activation, a Thr/Ser side chain is pulled toward the modified aspartate, and a Phe/Tyr side chain follows to fill the gap and changes from a semiexposed to a buried position. Concomitantly, mainly the β4-α4 loop of the Rec domain is changing its conformation. Much less is known about how these conformational changes elicited in the Rec domain are signaled downstream either to target proteins or to the output domain of full-length RRs. The structures of full-length CheB (Djordjevic et al., 1998), NarL (Maris et al., 2002), PrrA (Nowak et al., 2006), and members of the OmpR/PhoB subfamily (DrrB, DrrD) (Robinson et al., 2003) have been determined, but only in the nonactivated state. Distinct mechanisms of activation have been proposed, such as relief of active site obstruction (e.g., CheB) (Djordjevic et al., 1998) (PrrA) (Nowak et al., 2006), dimer or oligomer formation (e.g., PhoB) (Bachhawat et al., 2005), or both (NarL) (Maris et al., 2002).

PleD from *Caulobacter crescentus* is an unorthodox RR consisting of a Rec domain (D1) with the phosphorylatable aspartate, a Rec-like adaptor domain (D2), and the enzymatic DGC domain, also called the GGDEF domain according to a conserved sequence motif. The protein is intimately involved in the transition of the *Caulobacter* cells from the motile to the sessile form (Aldridge et al., 2003). To gain insight into the molecular mechanisms of catalysis and regulation exerted by DGCs, we have previously determined the crystal structure of PleD (Chan et al., 2004) (Figures 2A and 2C). The fold of DGC (PFAM00990; http://www.sanger.ac.uk/Software/Pfam/) closely resembles that of class III nucleotidyl cyclases, which include bacterial and eukaryotic adenylyl cyclases (ACs) (Chan et al., 2004). A recent review with a detailed comparison of DGC and AC has been published recently (Sinha and Sprang, 2006).

Enzymatic studies showed that pseudo phosphorylation of PleD by BeF_3^- results in a 35-fold increase of specific activity (R.P. et al., unpublished data). The nonactivated structure of PleD (Chan et al., 2004) suggests that this activation may occur via dimerization of the D1/D2 stem domains, which brings two DGC domains into proximity as a prerequisite for the condensation reaction to occur ("activation by dimerization"). At the same time, the structure showed that the c-di-GMP product crosslinks the DGC with the adaptor domain, suggesting, together with biochemical data, that the product allosterically inhibits the enzyme by hampering the productive encounter of the two DGC domains of the dimer ("inhibition by immobilization"). Later, the central role in feedback inhibition of the allosteric-binding site on the DGC domain (with a characteristic RxxD sequence motif) was demonstrated by mutagenesis, genetic screens, and sequence comparison, and an alternative allosteric model for the inhibition mechanism was proposed (Christen et al., 2006).

Here, we present the crystal structure of PleD after modification of the active aspartate with the phosphoryl analog BeF_3^- and compare it with the nonactivated structure (Chan et al., 2004). The modification induces a change in the relative arrangement of the two Rec domains within the monomer, resulting in the stabilization of the dimer that is the catalytically competent form (R.P. et al., unpublished data). Details about the binding mode of the substrate analog GTPαS/Mg^{2+} are elucidated, and possible catalytic mechanisms are discussed. Unexpectedly, a new, to our knowledge, and possibly general mode of noncompetitive product inhibition for DGCs in which c-di-GMP immobilizes the two DGC domains of the PleD dimer in a nonproductive arrangement is revealed.

RESULTS

Dimerization in Solution

Size-exclusion chromatography gave evidence that nonactivated PleD partly dimerizes in a concentration-dependent manner at high protein concentrations (Figure 1A). Most relevant, dimerization was enhanced by the addition of BeF_3^- and divalent cations (Mg^{2+} or Mn^{2+}) (Figure 1B), and the manganese cation was shown to be more efficient. In parallel, BeF_3^--induced dimerization has also been shown via chemical crosslinking, and it was shown that the dimeric fraction entirely contains the catalytic activity (R.P. et al., unpublished data).

To thermodynamically quantify the dimerization affinity, isothermal titration calorimetry (ITC) was performed. Figure 1C shows the heat peaks measured after injections of predominantly dimerized PleD into matching buffer; in the beginning of the titration, the dilution of the titrant is largest and causes the dissociation of the dimers. Since dimerization is exothermic in this case, heat is consumed for dissociation after each injection. With increasing concentration in the cell, more and more dimers persist, and the heat of dissociation decreases gradually. Figure 1D illustrates two pairs of such data sets obtained by normalization and baseline (Q_{dil}) correction of ITC curves with activated and nonactivated protein, respectively, on a logarithmic scale. Q_{dil} ranged from ~1 kcal/mol for the nonactivated PleD mutant to −6 and −3 kcal/mol for the activated protein, and they include dilution effects and slight pH or temperature mismatches of titrant and cell content. At first glance, it is seen that the activated protein dimerizes at a much lower concentration. Upon activation with BeF_3^-, the fitted dissociation constant, K_D, of dimerization decreased from about 100 μM to < 10 μM. Hereby, the latter value represents an upper limit, because, for this kind of experiment, the instrument was close to the detection limit. The enthalpy of dimerization is −10 kcal/mol for the nonactivated protein and is apparently somewhat less exothermic for the activated protein, suggesting that activation eliminates an entropic hindrance of dimerization.

Structural Changes Induced by Activation

To obtain the structure of activated PleD, crystallization was attempted with BeF_3^--modified protein. Crystals were obtained upon addition of c-di-GMP, which had been shown earlier to rigidify the multidomain protein by crosslinking an allosteric site of the DGC domain with a neighboring domain (Chan et al., 2004) and the substrate analog GTPαS/Mg^{2+} (Table 1). The pseudo phosphorylation at Asp53 in domain D1 resulted in a train of structural changes (Figures 2 and 3), ultimately leading to a dramatic tightening of the dimer interface of the $(D1/D2)_2$ stem compared to the nonactivated structure (Figure 2). Furthermore, but probably not as a consequence of activation, the arrangement of the DGC domains is drastically different from the nonactivated structure.

Asp53 of Rec domain D1 appears fully modified (Figures 3A and 3B) and closely resembles phospho-aspartate (Lewis et al., 1999), with a Be-O distance of 1.58 Å (restrained in refinement to 1.55 Å) and a C_γ-O_δ-Be-F_1 dihedral *cis* conformation. The moiety forms four H bonds with the binding pocket and contributes to the coordination of the adjacent Mg^{2+} ion. The modification results in a restructuring of the β4-α4 loop, with Thr83 moving by more than 3 Å relative to the position in the nonactivated state to form an H bond with the BeF_3^- moiety (Figures 3A and 3B). The vacated space, in turn, is claimed by Phe102,

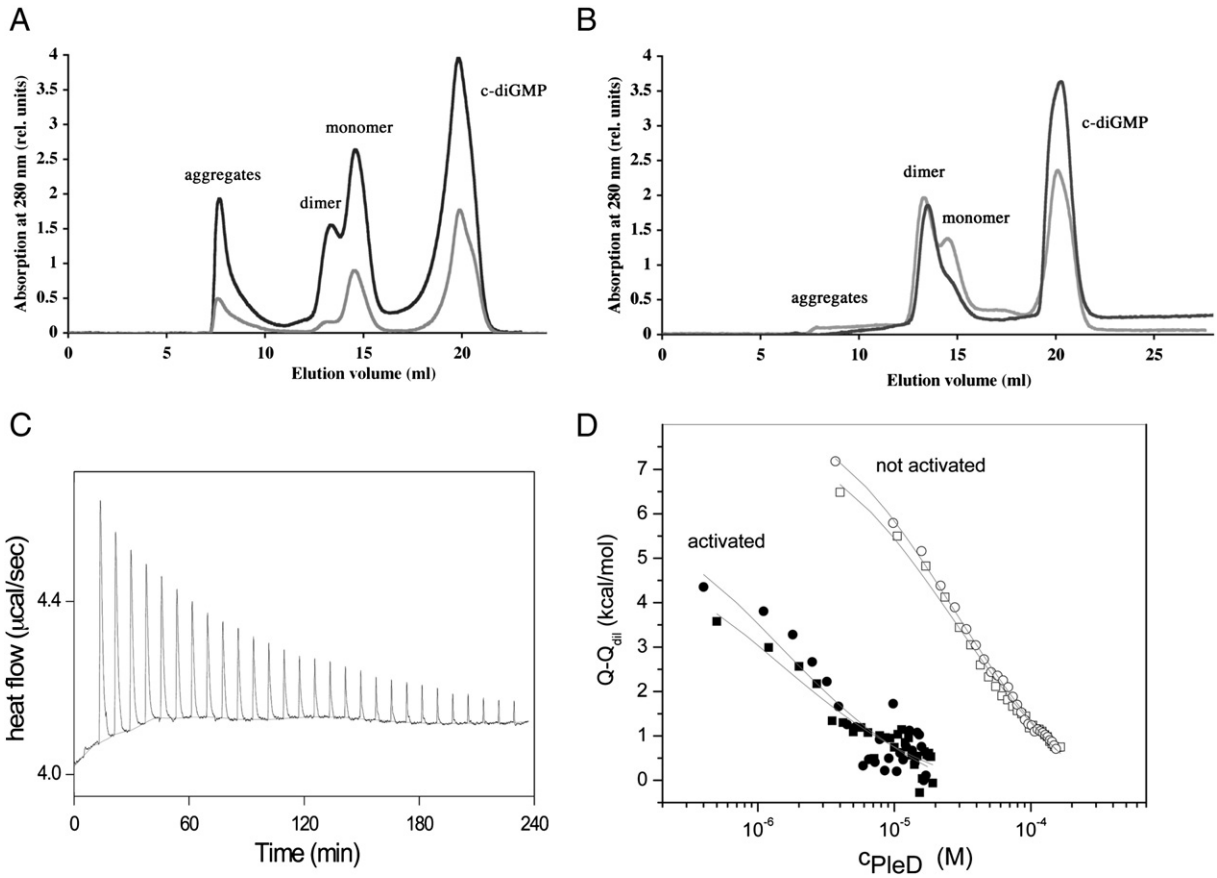

Figure 1. Size-Exclusion Chromatography Elution Profiles and Isothermal Titration Calorimetry of Purified PleD Mutant R313A

(A–D) This mutant with unmodified dimerization domains had been chosen for technical reasons (availability of material). (A) Elution profiles of nonactivated PleD at a protein concentration of 33 µM (gray) and 66 µM (black). (B) Elution profiles of BeF_3^--modified PleD (66 µM) in presence of 10 mM $MgCl_2$ (gray) and 1 mM $MnCl_2$ (black). Note that c-di-GMP is released and separated from the protein during the runs. (C) The primary ITC data for a dilution experiment (initial PleD concentration = 0.86 mM) with nonactivated PleD. (D) The integrated two ITC data sets for the activated (solid symbols) and nonactivated (open symbols) PleD mutant, after subtraction of the baseline heats, Q_{dil}, obtained by model-based extrapolation of the curves to high concentrations. The curves illustrate the best fits with shared K_D values of 100 µM (nonactivated) and 10 µM (activated). Due to the noisy data, the latter value represents an upper limit.

which changes its side chain conformation from gauche+ to *trans* to become buried; part of the β5 main chain (residues 102–104) moves up to 2 Å.

Domain D1 interacts closely and in a pseudo two-fold symmetric manner with the adaptor domain D2 across the α4-β5-α5 faces of both domains. Activation results in a domain rotation/shift of 14°/6 Å of D2 relative to D1 and a massive repacking of the domain interface (Figure 3A). In Figures 3C and 3D, the D1/D2 interface is displayed in its two states. While most of the contacting D1 residues stay in touch with the D2 domain, Arg91, Val110, and Ile251 contribute to the interface only in the nonactivated state, and residues Arg88, Ile92, Leu95, Val241, Gln259, and Ala263 contribute only in the activated state. Amazingly, the three interdomain salt bridges (Asp108-Arg237, Arg115-Asp250, Asp101-Arg264) are not disrupted during the transition, although the partners move up to 7 Å with respect to each other. However, upon activation, Asp257 swaps its ion-pair partner Arg91 for Arg88. Upon activation, the hydrophobic contact patch around Met111, Ala114, Met240, and Leu244 becomes repacked, and an additional apolar contact is formed that involves Ile92, Leu95, and Ala263 (Figures 3C and 3D).

On the quaternary level, in both crystal structures, the Rec and the adaptor domains form a dyad symmetric $(D1/D2)_2$ "stem" with the equivalent domains of a second monomer (Figure 2). Since both domains contribute to the interchain interface, it is obvious that the relative repositioning of the domains within each chain also has consequences on the quaternary structure. The weak dimer interface observed in the nonactivated structure (Chan et al., 2004) is greatly tightened upon activation (Figures 2C and 2D), and the buried accessible surface areas per monomer (ΔASA) increased from 900 $Å^2$ to 1436 $Å^2$.

In both states, the interchain contacts between D1 and D2 are formed in an isologous, i.e., two-fold symmetric manner. In the nonactivated structure, there is only a small contact patch around Tyr26 resulting in a discontinuous

Table 1. Data Collection and Refinement Statistics of Activated PleD in Complex with c-di-GMP and GTPαS

Data Collection	
Space group	$P2_12_12$
Cell dimensions	
a, b, c (Å)	128.9, 132.6, 88.4
Resolution (Å)	30–2.71 (2.85–2.71)
R_{merge} (%)	9.8 (43.6)
I/σ(I)	10.2 (1.9)
Completeness (%)	95.0 (78.0)
Redundancy	2.9 (2.4)
Refinement	
Number of reflections	39,043
R_{work}/R_{free}	21.7/25.4
Number of atoms	
Protein	7,012
Ligands	272
Water	14
B factors (Å^2)	
Protein	41.0
Ligands	43.7
Water	29.2
Rmsds	
Bond lengths (Å)	0.011
Bond angles (°)	1.5

Data in parentheses belong to the outer resolution shell.

interface (Figure 4A). While this contact is maintained in the activated structure, a multitude of additional interactions are formed involving the α1, β2, β3, α5 face of D1 and the α3, α3-β3, α5 face of D2 (Figure 4B). Three salt bridges are formed between the subunits, and there is a sulfate ion on the two-fold symmetry axis at the center of a basic cluster formed by Arg117 and Arg121 with their symmetry mates (Figure 4B). In addition, there are a few polar interactions and a small hydrophobic cluster formed by Leu124 and Val125 and their symmetry mates.

Upon activation, the α5 helices of the stem domains become extended by 4–5 residues at the C terminus. It is these helices that experience the largest change in relative interchain distance, moving from a closest distance of about 10 Å to direct van der Waals contact (Figures 4A and 4B). Together with their symmetry mates, the C-terminal thirds of the four α5 helices form a parallel α helix bundle in the dimer (Figure 2B).

Active Site

To gain further insight into the catalytic action of DGCs, the substrate analog GTPαS and Mg^{2+} had been added to the crystallization set-ups. In the activated structure, both active sites of the DGC domains, which face away from each other (see below), are occupied by the ligands. Figure 5 shows that the β- and γ-phosphates are tightly bound and form two H bonds to main chain amides of the short P loop between strand β1 and helix α1 and ionic interactions to Lys442, Arg446, and a putative Mg^{2+} ion (named metal B in analogy to the situation in adenylate cyclases [Tesmer et al., 1999]). The cation is additionally coordinated by main chain carbonyl 328 of the P loop, both carboxylate oxygens of Asp327, and Glu370, OE1. In one subunit of the dimer (subunit A), a second putative Mg^{2+} ion (metal A) is bound from another side to the same two side chains, interacting with atoms Asp327, OD2 and Glu370, OE2, respectively. Consistent with the structure, mutation of Asp327 to Ala resulted in a complete loss of enzymatic activity, as has been seen previously for mutant E370Q (Christen et al., 2006). The elongated density of the omit map (Figure 5) and the elevated B factor of the ion (52 Å^2) possibly indicate alternative positions for this ion. Neither the α-thiophosphate nor the ribose moiety are bound to the protein by specific interactions, resulting in comparatively high B values (~60 Å^2). The guanine moiety, in contrast, is well adopted, forming H bonds with Asn335 and Asp344 of the guanine-binding pocket, also already identified in the nonactivated protein-product complex (Chan et al., 2004).

Allosteric Product Binding

Compared to the previously determined nonactivated structure of PleD, the DGC domains adopt a drastically different position with respect to the stem domains. While, in the previous structure, the weak D2/DGC interface is strengthened by a bound c-di-GMP dimer that effectively crosslinks the domains (Figure 2A), in the present structure, this interface is completely disrupted and the DGC domains are swung out to form a two-fold symmetric c-di-GMP-crosslinked dimer (Figure 6). The difference in the relative orientation of the DGC domain with respect to the stem is probably not a direct consequence of Rec modification, since, assuming a flexible D2-DGC linker, a change of the crosslinking mode appears to be structurally feasible in either state. Thus, both domain organizations would occur in thermodynamic equilibrium in solution.

C-di-GMP forms dimers with the four guanyl bases stacked and intercalated as in small-molecule crystals (Egli et al., 1990; Liaw et al., 1990). Figure 6B shows that this form is found bound to the allosteric site. Two guanyl bases interact with DGC residues Arg359, Asp362, and Arg390 (primary I site, I_p), whereas the neighboring third base is bonded to Arg313 of the adjacent DGC domain (secondary I site, $I_{S,DGC}$). Due to symmetry, there are two isologous crosslinks within the DGC dimer (Figure 6). The dimer interface (with a ΔASA of 517 Å^2 that increases to 1044 Å^2 upon ligand binding) is exclusively hydrophobic and involves Ala360, Ile361, Pro377, and the hydrophobic part of the Ser309 side chain. Noteworthy, in the nonactivated structure, a c-di-GMP dimer is bound to I_p in exactly the same way, but it crosslinks with the third base and a phosphate moiety to Arg148 and Arg178 of the D2 domain ($I_{S,D2}$).

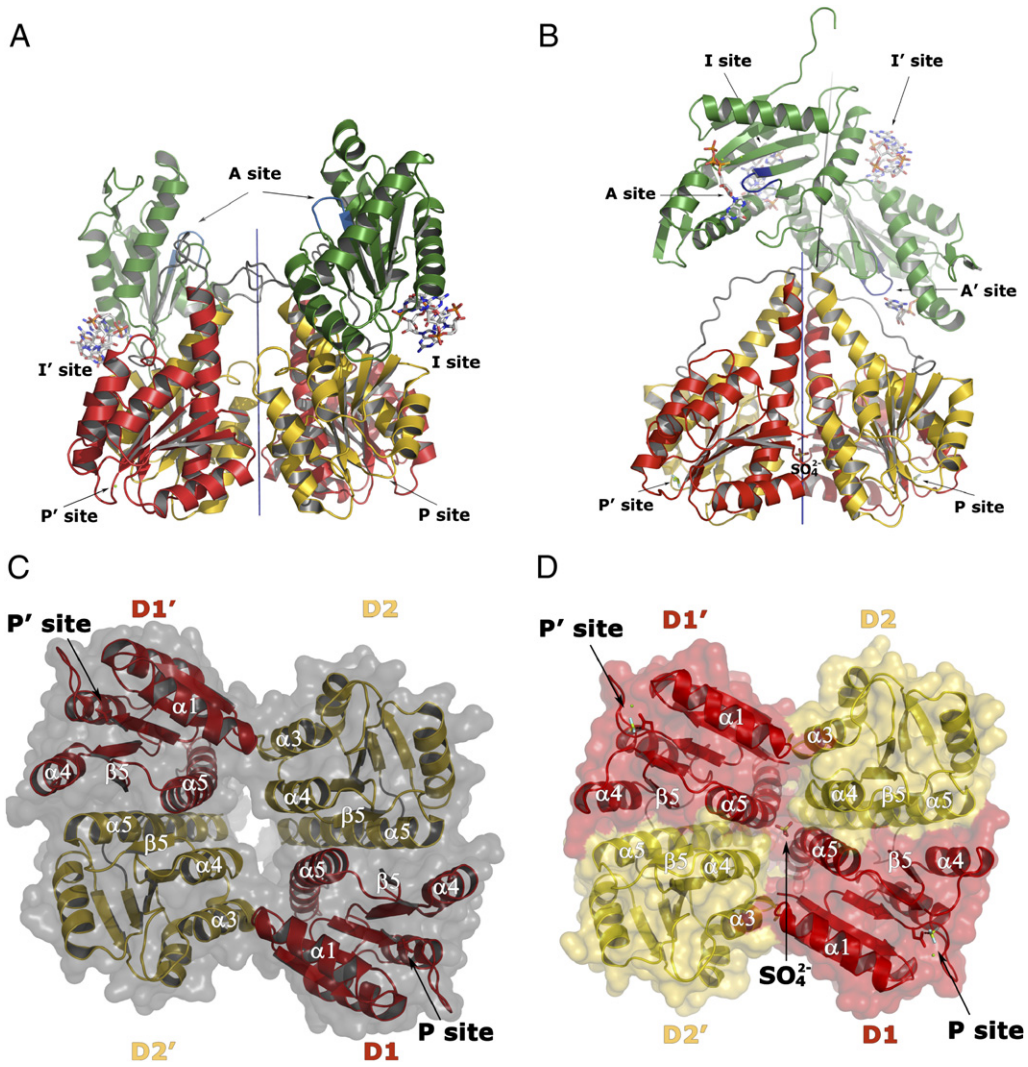

Figure 2. Ribbon Diagrams of the Dimeric Crystal Structures of Nonactivated PleD and BeF_3^--Activated PleD

(A–D) In (A) and (B) the view is perpendicular to the two-fold axis of the stem. In (C) and (D), the view is rotated by 90° around a horizontal axis with respect to the top panels, showing the bottom view of the $(D1/D2)_2$ stem with the DGC domains in the rear clipped off for clarity. The domains are colored in red (Rec domain D1), yellow (adaptor domain D2), and green (enzymatic domain DGC, with the GGEEF signature motif highlighted in blue). The disordered parts of the interdomain linkers are shown in gray. Labels with a prime indicate symmetry-related elements. The two-fold symmetry axes are shown as thin, straight lines. (A and C) Nonactivated PleD (Chan et al., 2004) is associated to a loose dimer. The active sites (A sites) are occupied by c-di-GMP, which crosslinks to an adjacent dimer (not shown). Intercalated $(c\text{-di-GMP})_2$ dimers are bound to allosteric inhibition sites I and I′. Each inhibition site is comprised of a primary inhibition site on DGC (I_p; Arg359, Asp362, Arg390) and a secondary site on the adaptor domain ($I_{s,D2}$;R148, R178). (B and D) In the activated structure, the phosphorylation site (P site) is modified by BeF_3^- and Mg^{2+}, and the active site (A site) harbors GTPαS/Mg^{2+}. $(C\text{-di-GMP})_2$ dimers are bound to the dyad-related sites I and I′. Each site is comprised of the primary I_p site, as in the nonactivated structure, and a secondary I site of the symmetry-related DGC ($I_{s,DGC}$; R313; also see Figure 6). The two A sites face in opposite directions, rendering the enzyme catalytically incompetent.

Feedback Inhibition Probed by Mutagenesis

PleD shows noncompetitive product inhibition with a K_i of about 0.5 μM (Chan et al., 2004) (Table 2). Crosslinking of the DGC domain to the D2 domain, as seen in the crystal structure of nonactivated PleD, has been proposed to be the mechanism of product inhibition in PleD, since this would prevent the productive encounter of the two GTP-loaded enzyme domains (Chan et al., 2004). To test the "inhibition by domain immobilization" hypothesis, pertinent PleD mutants have been analyzed recently (Christen et al., 2006). Mutations of primary I site (I_p) residues were, apart from R390A, largely deleterious for activity and, thus, inconclusive. Mutation R390A, however, showed a considerably increased K_i. Truncation of the secondary I site residues on D2 ($I_{s,D2}$; mutant R148A/R178A), on the other hand, did not affect feedback inhibition.

Here, we applied a photometric pyrophosphate assay to reinvestigate this $I_{s,D2}$ mutant and to probe the role of the secondary $I_{s,DGC}$ site (Arg313). As can be seen from Table 2, mutating the $I_{s,D2}$ or the $I_{s,DGC}$ site alone had a

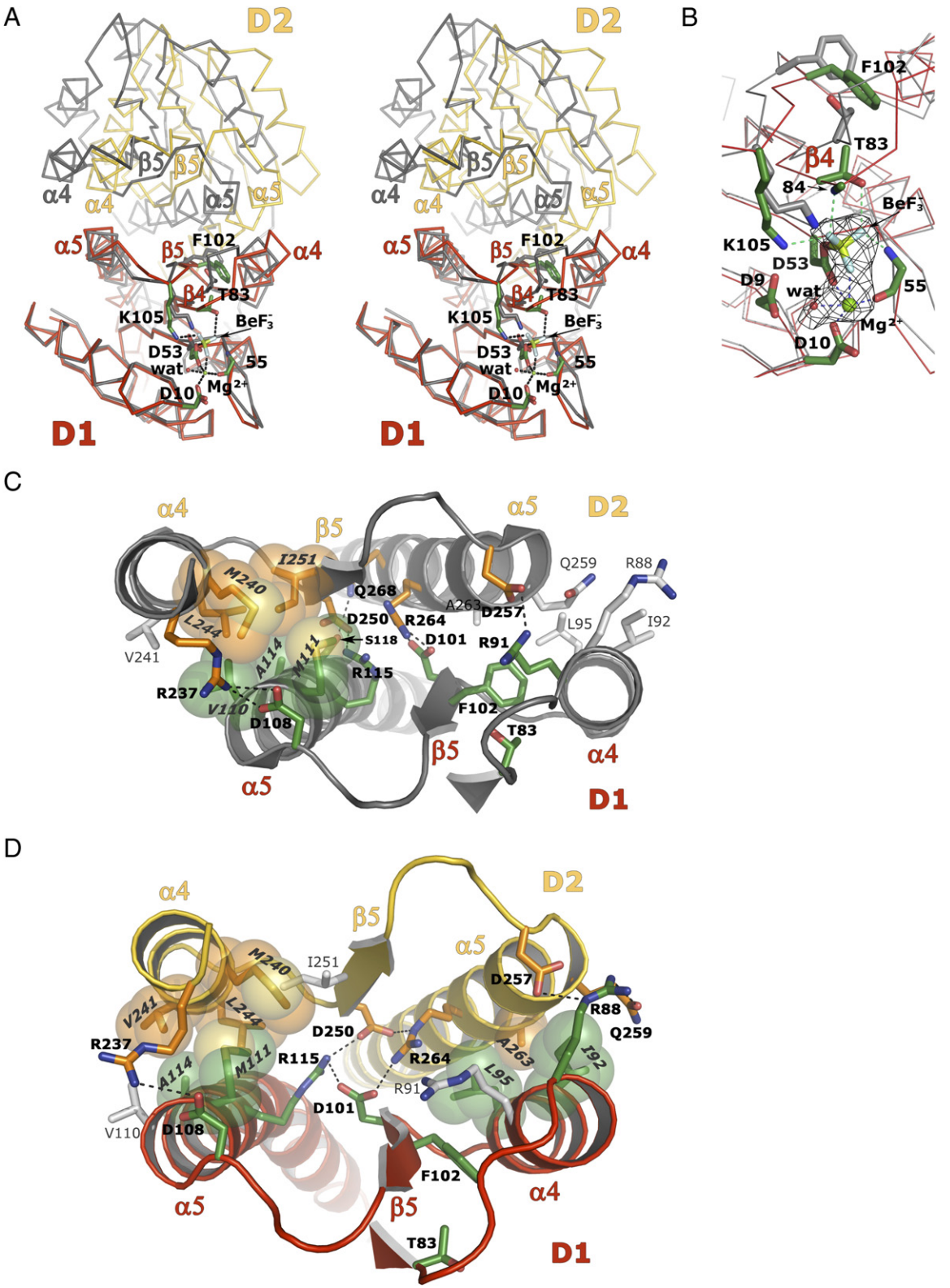

Figure 3. Structural Changes Invoked by BeF_3^- Modification of Asp53

(A) Comparison of the Cα traces of the D1/D2 PleD stem in its activated (D1, red; D2, yellow) and nonactivated (gray) conformation after superposition of the D1 domains. Residues of the acidic pocket as well as Thr83 and Phe102 are shown in full.

(B) Blow-up of the superimposed D1 domains around the activation site; residues involved in pseudo phosphorylation are shown in full. The omit map for Asp53-BeF_3^- and the associated Mg^{2+} ion is depicted at 3α.

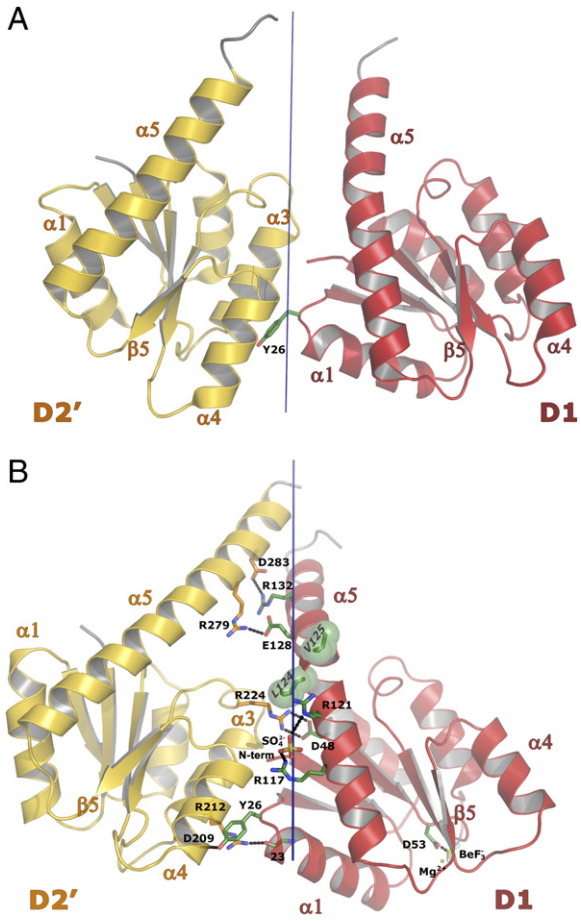

Figure 4. Intermonomer D1/D2′ Contact before and after Activation

(A and B) In the dimeric stem, all shown contacts occur twice due to the two-fold symmetry. Interface residues are shown in full. (A) In nonactivated PleD, the interaction is restricted to a small contact patch around Tyr26. In (B) activated PleD, there is a multitude of polar and ionic interactions and an apolar contact between Leu124, Val125 (green spheres,) and the corresponding residues of the symmetry-related D1′ (not shown). A putative sulfate ion is found on the symmetry axis crosslinking Ag117 and Arg121 with their symmetry mates.

moderate effect on the inhibition constants, with a 10-fold and 2-fold increase, respectively. Our values deviate slightly from those measured by Christen et al. (2006) for wild-type and R148A/R178A PleD, possibly because their data had been measured by a different technique (thin-layer chromatography). Furthermore, the published K_i values were actually IC_{50} values. Truncating both secondary I sites in the triple mutant R148A/R178A/R313A increased the K_i by more than 60-fold. Interestingly, it was not possible to inhibit this mutant completely, with the inhibited state showing a residual k_{cat}' rate constant of about 5% of k_{cat} (Table 2; Figure S2D, see the Supplemental Data available with this article online). All mutants, but in particular those involving $I_{s,D2}$ residues, showed considerably elevated activity (Table 2). This may be due to a decreased dimerization K_D of the nonactivated mutant proteins.

The K_D of c-di-GMP binding to the triple mutant is about 4 μM (ITC measurement, data not shown) and, thus, is increased by only a factor of about 10 with respect to PleD wild-type (R.P. et al., unpublished data). This affinity most probably is due to c-di-GMP binding to the uncompromised I_p site. In summary, the data indicate that the two immobilization modes operate redundantly, i.e., the integrity of only one of the I_s sites is required for noncompetitive product inhibition, presumably via domain crosslinking.

DISCUSSION

DGCs play a central role in bacterial c-di-GMP signaling. Therefore, their action, synthesis of the secondary messenger, must be tightly controlled (Christen et al., 2006). Comparison of the structures of nonactivated and activated PleD allows us to propose the mechanisms of activation by phosphorylation and, unexpectedly, suggests two redundant modes of feedback inhibition. For a schematic overview of the various structural states of PleD, see Figure 7. Furthermore, the binding mode of the substrate analog GTPαS gives insight into the catalytic mechanism of the cyclization reaction.

Activation

It has recently become apparent that BeF3-modified Rec domains of RR transcription factors of the OmpR/PhoB family form two-fold symmetric homodimers (Bachhawat et al., 2005; Toro-Roman et al., 2005a, 2005b). Since their DNA-binding domains bind cooperatively to their target sequences, it was suggested that protein dimerization is the mechanism of activation. In some cases, the active dimer structure was also seen in crystals of the native protein (Toro-Roman et al., 2005a, 2005b), which may, however, be of no physiological relevance considering the high protein concentration needed for crystallization.

In PleD, the signal generated by pseudo phosphorylation of Asp53 is transduced to the α4-β5-α5 face, where it promotes the D1/D2 rearrangement, which, in turn, facilitates dimerization. As in other Rec domains, the conserved Phe/Tyr at the center of this interface follows the movement of a Thr/Ser and changes its rotameric state. The movement of Phe102 is compensated by a slight twist of the C terminus of helix α4, allowing residues Ile92 and Leu95 to make apolar interdomain contacts with Ala263. Together with other rather subtle differences at the α4-β5-α5 face of D1 a substantial domain rearrangement is induced (Figure 3A). It is unlikely that these rearrangements are caused by crystal packing, since, in the loosely

(C and D) Close-up view of the D1/D2 interface in the (C) nonactivated and (D) activated state showing the quasi-two-fold symmetric interface. Both domains contribute their α4-β5-α5 face. The viewing direction is along the quasi-dyad. All residues of the D1/D2 interface as well as Thr83 and Phe102 are shown in stick and sphere representation for polar and apolar residues, respectively. Residues, which do not interact in one state, but do so in the other, are shown in white.

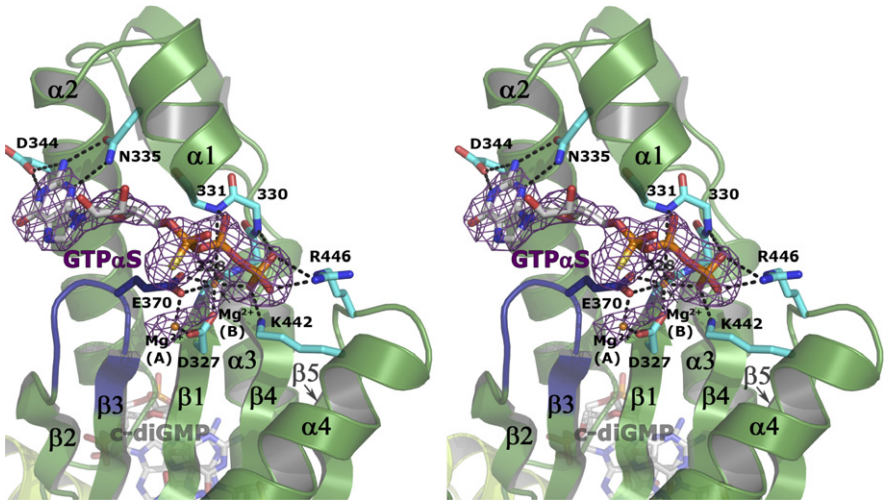

Figure 5. Substrate Analog GTPαS and Mg^{2+} Bound to the Active Site of PleD

The omit map for the ligands is contoured at 3σ. The DGC domain is shown in ribbon representation; the GGEEF signature hairpin is shown in dark blue, and all interacting residues and the P loop main chain (residues 328–331) are shown in full. $(c\text{-di-GMP})_2$ bound to the I_p site of the DGC domain can be seen in the rear.

packed crystals (V_M = 3.8 Å^3/Da), the crystal contact areas are more than 2-fold smaller than the dimer interface.

Interestingly, the two PleD Rec domains of a given chain interact quasi-two-fold symmetrically and in a very similar way as what is observed for the homodimerization of Rec domains of the OmpR/PhoB subfamily. While the α4-β5-α5 face is the interaction surface in both cases, the similarity even extends to the residue level. In PleD, Asp101/Arg115 and Asp250/Arg264 form two quasi-isologous interdomain salt bridges at the center of the interface (Figures 3C and 3D), whereas homologous residues form isologous interchain salt bridges in the Rec domains of the OmpR/PhoB family (e.g., Asp99/Arg113 for ArcA) (Toro-Roman et al., 2005a).

DGCs catalyze the condensation of two identical substrates (GTP) to form the two-fold symmetric c-di-GMP product. Since the DGC domain binds only one substrate, two such domains are needed for catalysis, as depicted in the mechanistic model of Figure 7 (state 4). Control of dimerization allows for simple and efficient regulation of the catalytic activity, as the reaction type for the encounter of substrate-loaded DGC domains is changed from bi- to unimolecular. At the high protein concentration of 20 μM used in the enzymatic assays (Table 2), dimerization of nonactivated PleD with a K_D of about 100 μM is not negligible, explaining the observed constitutive activity. The physiological PleD concentration is not known and may vary within the cell. But, clearly, activation by reduction of the dissociation constant, K_D, will be most effective at protein concentrations well below the K_D of nonactivated PleD. Indeed, it has been shown that, at a lower protein concentration of 5 μM, the catalytic rate is enhanced by a factor of 35 upon BeF_3^- modification, and that it is the dimeric species that carries the activity (R.P. et al., unpublished data).

For WspR from *Pseudomonaas fluorescens*, which is a DGC with a single N-terminal Rec domain, a more indirect dimerization mechanism, with phosphorylation relieving the dimer interface obstruction caused by the effector domain, has been proposed (Malone et al., 2007). For RRp1 from *Borrelia burgdorferi*, which has the same Rec-DGC domain organization, phosphorylation-dependent cyclase activity has been demonstrated (Ryjenkov et al., 2005). Thus, in these cases, a second Rec-like domain such as the adaptor domain of PleD appears to be dispensible for dimerization, and it may serve an additional regulatory function in RRs with a Rec-Rec-DGC domain composition (see below). How DGCs without Rec domains are activated remains to be investigated. Several of them may be constitutive dimers such as DgcA (CC3285) from *C. crescentus* with its putative N-terminal coiled-coil domain (P.W., unpublished data).

Catalysis

The active site of the DGC domain of PleD is identified by the bound substrate analog GTPαS. It consists of well-defined subsites for the β- and γ-phosphates and for the guanine base (Figure 5), which explains the observed substrate specificity (Chan et al., 2004; Paul et al., 2004). The structural similarity of the DGC domain to adenylate cyclase (AC) and DNA polymerase (POL) has been pointed out (Chan et al., 2004). From this work, it is apparent that the similarity also extends to the mode of substrate binding as far as the position of the terminal phosphates close to the P loop, the presence of metal B, and its coordination by the phosphates and two invariant carboxylates (D327 and E370 in PleD) are concerned. Metal site A is also occupied in one of the subunits (Figure 5), but the α-phosphate is not in coordinating distance as in the bacterial AC CyaC (Steegborn et al., 2005) and in POL

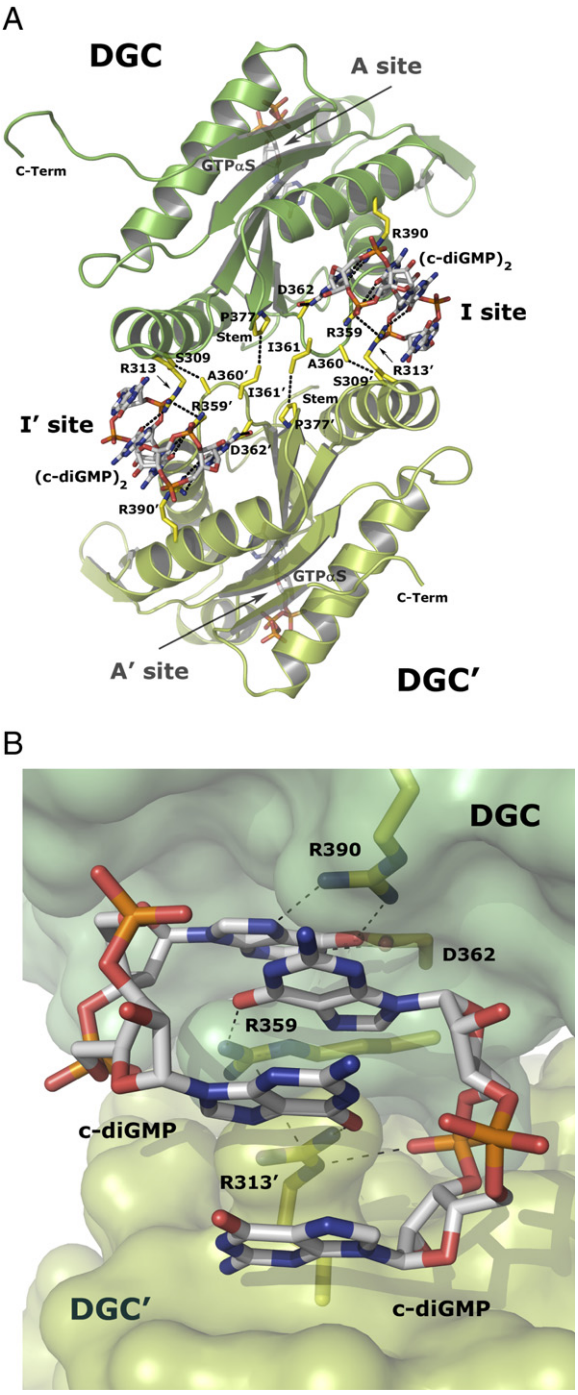

Figure 6. Crosslinking of the DGC Domains by c-di-GMP

(A) Ribbon diagram of the DGC dimer along its symmetry axis; both $(c\text{-di-GMP})_2$ ligands and interacting residues are shown in full. The $(c\text{-di-GMP})_2$ ligands are bound to the I site (I_P site and the $I_{s,DGC}$ site of the adjacent subunit).

(B) Close-up view of the intercalated $(c\text{-di-GMP})_2$ ligand, which crosslinks the two DGC domains (dark- and light-green surface representation) by binding to the I_p (Arg359, Asp362, Arg390) and the $I_{s,DGC}$ (R313′) site of the adjacent domain.

(Doublie et al., 1998). This may be caused by the thiol modification of the ligand or the absence of the second substrate. Modeling shows that moderate torsional adjustments can bring the α-phosphate in coordinating distance to metal A, with an orientation ready for in-line attack onto the P_α-P_β diester bond. This can occur without compromising binding of the terminal phosphates or the guanine.

The role of the conserved Glu371 in DGCs (Figure S1) has not been clarified, but it may coordinate metal A transiently and/or serve as a proton acceptor for the incoming 3′-hydroxyl of the other subunit. Indeed, mutagenesis has shown that Glu371 is as indispensable for catalysis as are the magnesium ligands Glu370 (Christen et al., 2006) and Asp327 (data not shown). Another conserved residue in the active site is Lys332, whose side chain amino group can easily adopt a position from which it could stabilize the charge of the pentavalent phosphoryl transition state and the pyrophosphate leaving group (Figure S1). The same role has been postulated for the nonhomologous Arg1150 in CyaC (Steegborn et al., 2005).

To form the catalytically competent enzyme-substrate complex (Michaelis-Menten complex), two substrate-loaded DGC domains have to line-up in antiparallel orientation, such that the 3′-hydroxyl groups of the bound substrates are brought in close proximity to the α-phosphate of the other GTP molecule and such that they are properly positioned to perform an intermolecular in-line nucleophilic attack onto P_α from the side opposing the susceptible P_α-P_β diester bond. Modeling shows that this can be achieved without clashes in a dimeric arrangement, in which helix α4 of one domain contacts the small β sheet (β0, β0′) of the symmetry-related domain (Figure S1). The interface carries a number of ionic side chains that probably are involved in intermolecular salt bridges. The model of the $(DGC)_2$-c-di-GMP product complex obtained after only minor rearrangements of the reactive groups (Figure S1B) is different from that observed experimentally in nonactivated PleD (Chan et al., 2004), where c-di-GMP crosslinks A sites of adjacent dimers. This is due to a difference in the position of the ribose and α-phosphate moieties relative to the protein, whereas the guanine base is bound in the same way. The orientation of the product in the active site of nonactivated PleD is most probably enforced by the artifactual, ligand-mediated dimer-dimer association in the crystal.

The close resemblance of the constellation of reactive groups and metal ions in the modeled PleD Michaelis-Menten complex with that in AC and POL suggests that the same two-metal-assisted mechanism for phosphodiester formation as suggested for ACs (Tesmer et al., 1999) and for POLs (Steitz, 1999) is operational in DGCs. More kinetic and mutagenesis experiments have to be performed to reveal the precise catalytic mechanism of DGCs.

Feedback Inhibition

DGCs exhibit exquisite noncompetitive product inhibition, as demonstrated biochemically for PleD (Chan et al., 2004; Paul et al., 2004) and for DgcA from *C. crescentus*

Table 2. Kinetic Data of Nonactivated Wild-Type and Mutant PleD

	Wild-type PleD	PleD R148A/R178A	PleD R313A	PleD R148A/R178A/R313A
IC_{50} (μM)	7 ± 2	17 ± 4	9 ± 2	30 ± 5
K_i (μM)	0.5[a]	5	0.9	33
K_s (μM)	26	20[a]	21	25
k_{cat} (μM c-di-GMP/[s · μM PleD])	$9.0 \cdot 10^{-4}$	$1.5 \cdot 10^{-2}$	$4.0 \cdot 10^{-3}$	$1.6 \cdot 10^{-2}$
k_{cat}' (μM c-di-GMP/[s · μM PleD])	0[a]	0[a]	0[a]	$8.1 \cdot 10^{-4}$

IC_{50} values represent experimental values with estimated standard deviations based on two measurements at GTP concentrations of 100 μM and 500 μM. The concentration of the protein was 20 μM. The other kinetic parameters have been obtained by fitting numerical simulations to the time course of c-di-GMP concentration at various inhibitory concentrations (Figure S2). In the simple kinetic scheme, enzyme and substrate as well as enzyme and product are in thermodynamic equilibrium, with dissociation constants of K_s and K_i, respectively, with the product binding noncompetitively to an allosteric site. Also, product and substrate binding are assumed to be independent of each other. k_{cat} and k_{cat}' are the catalytic rate constants of substrate turnover for noninhibited and inhibited protein, respectively. The fitted values for the on-rate constants of substrate and product ranged between 100 s^{-1} and 350 s^{-1}. It should be noted that the fits for PleD wild-type and mutant R148A/R178A were poor (Figures S2A and S2B), and, hence, the corresponding parameters not very well determined. This may be due to the simplicity of the kinetic model.
[a] Parameter was fixed in simulation.

(Christen et al., 2006), and, based on conserved I_p sites, this is expected to be the case for the majority of DGC domains (Christen et al., 2006). Feedback inhibition prevents futile GTP consumption and probably defines an upper ceiling for the concentration of the second messenger c-di-GMP in the bacterial cell. Christen et al. (2006) showed that the allosteric I_p site is crucial for binding and product inhibition and suggested that communication between the

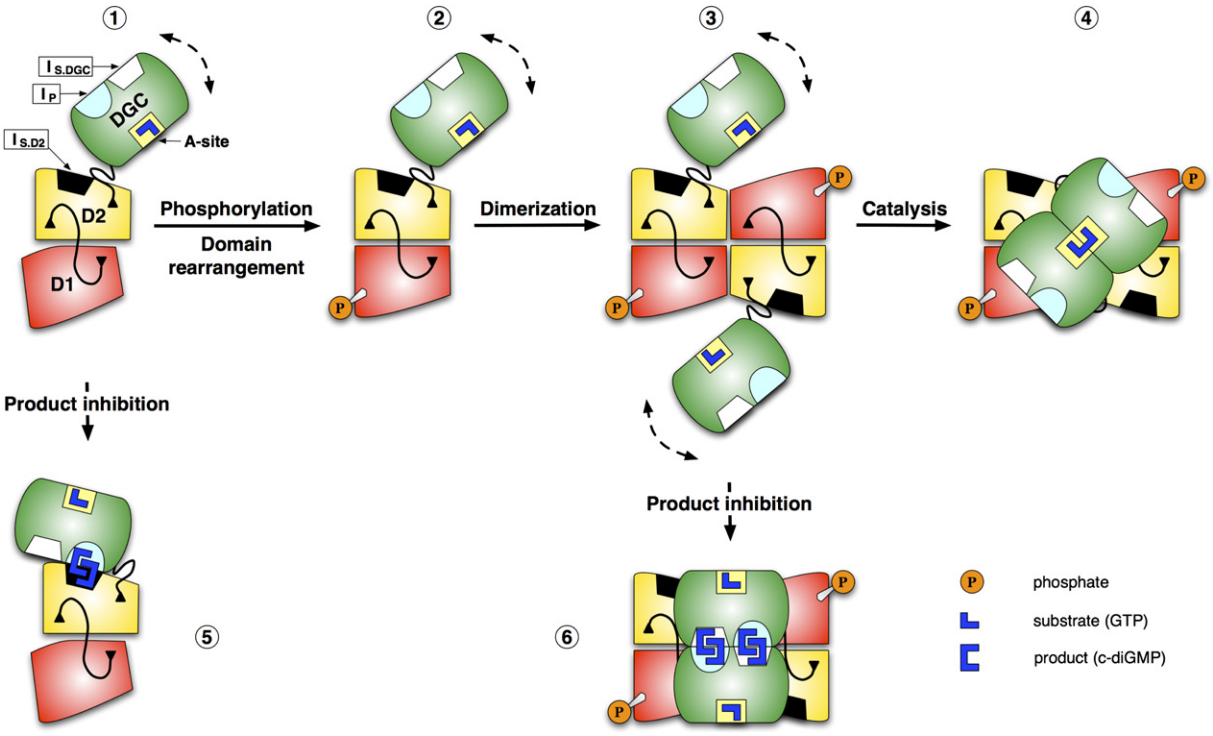

Figure 7. Mechanistic Model of PleD Regulation
The model is adapted from Chan et al. (2004). The DGC domain (green) is connected via a flexible linker to the stem (receiver domain D1 [red] and adaptor domain D2 [yellow]) and is supposed to be mobile relative to it. (Upper row) Activation. Phosphorylation of domain D1 leads to a rearrangement of the stem domains, which, in turn, allows for formation of a tight dimeric stem (3). The dimeric arrangement is a prerequisite for an efficient and productive encounter of the two substrate-loaded DGC domains to form the c-di-GMP product (4). (Lower row) Product inhibition. Dimeric product molecules, $(c\text{-di-GMP})_2$, can crosslink the primary inhibition site on DGC, I_p, with a secondary binding site either on D2, $I_{s,D2}$ (5) or on the adjacent DGC domain, $I_{s,DGC}$ (6). The former structure has been observed experimentally with nonactivated PleD (Chan et al., 2004), the latter structure is presented in this report. In both cases, the DGC domains become immobilized, and the active sites are hampered from a productive encounter. Note that a possible direct communication between I_p and A sites (Christen et al., 2006) is not depicted.

I_p site and the active site of a DGC domain could cause the observed noncompetitive product inhibition. However, in the nonactivated structure (Chan et al., 2004), the enzymatic product in the form of two intercalated c-di-GMP molecules was found to crosslink the I_p with the $I_{s,D2}$ site on the adjacent D2 domain (Figure 7, state 5). Therefore, an "inhibition by domain immobilization" mechanism, in which domain crosslinking by c-di-GMP would prevent productive encounter of the two enzymatic domains of the dimer, was proposed. Indeed, $(c\text{-di-GMP})_2$ can be regarded as a multivalent ligand that offers, among other features, the O6-N7 edges of its four guanyl bases for specific pairing with arginine guanidyl groups, as observed in DNA-protein interactions. In nonactivated PleD, the ligand crosslinks the well-defined and well-conserved (Christen et al., 2006) I_p site on the $\alpha 2$-$\beta 2$ corner of DGC (formed by Arg359, Asp362, Arg392) with arginines 148 and 178 of D2 ($I_{s,D2}$).

In the present structure, a similar mechanism can be deduced. In this mechanism, the dimeric ligand is again bound to the I_p site, but its other valency crosslinks to a hitherto unrecognized, to our knowledge, secondary site on the adjacent DGC domain of the dimer ($I_{s,DGC}$). As a result, the DGC domains interact in a nonproductive manner with the two A sites, which point away from each other (Figure 2B). Our functional analysis of pertinent mutants (Table 2) suggests that domain immobilization might indeed contribute to feedback regulation, and that the two inhibition modes operate redundantly (Figure 7, states 5 and 6). The advantage of redundancy in this context is not clear, but we note that efficient DGC-DGC crosslinking obviously can operate only after dimerization, while D2-DGC crosslinking occurs within the nonactivated monomer. Why the triple mutant is not fully active upon c-di-GMP binding, but rather switches to a slower rate (Table 2), remains to be investigated. This may be due to the residual binding capacity of the mutated I_s sites, the existence of additional I_s sites with low affinity, or a change of active site structure and/or dynamics upon allosteric product binding to the I_p site, as suggested by molecular simulations (Christen et al., 2006).

The relevance of feedback inhibition has been discussed before upon recognizing that the $R_{359}xxD_{362}$ motif of the I_p site is largely conserved (Christen et al., 2006). It is present in 59% of all GGDEF domain sequences of the current PFAM release (5200 sequences) that have an intact GGD(E)EF motif and are, therefore, putative DGCs. A large part of these seem to operate via c-di-GMP crosslinking of I_p with an $I_{s,DGC}$ site, as observed in the present PleD structure. This can be inferred from the fact that 64% of the DGC sequences with the RxxD motif show an arginine at position 313 of helix $\alpha 0$ or at a position one turn of the helix farther up (positions 316 and 317), from where the long side chain probably could also reach the ligand. Covariation calculations show a significant correlation of 0.45 (0.32, 0.61) for simultaneously finding the RxxD motif and an arginine at position 313 (316, 317). Of the subset of 19 DGCs for which guanylate cyclase activity has been shown experimentally (see Figure S4 in Christen et al. [2006]), 14 display the RxxD motif of the I_p site, and all but one display an arginine residue at one of the secondary positions.

This implies that catalytic domain immobilization by DGC-DGC crosslinking is a rather common feedback inhibition mechanism of DGCs and does not rely on secondary inhibition sites on other domains. This autonomy of the DGC domain has probably been an advantage in evolution to conserve feedback inhibition. Interestingly, feedback inhibition is also observed in the prototype of a "single-domain" DGC, DgcA from *C. crescentus*, whose sequence exhibits both I_p and $I_{s,DGC}$ sites as well as a small N-terminal extension of possibly coiled-coil structure for dimerization (Christen et al., 2006).

The multivalency of the second messenger c-di-GMP appears perfectly suited for signal transfer. Here, we showed evidence that it can be utilized for domain crosslinking, which elicits large structural changes and which may well also work for downstream signaling processes. Interestingly, c-di-GMP binds to the N terminus of the PilZ effector domain (Christen et al., 2007), i.e., to a strategic position where it could control domain arrangement in multidomain targets carrying this domain. The identification of additional c-di-GMP effector proteins will reveal to what extent this notion can be generalized.

EXPERIMENTAL PROCEDURES

Mutagenesis, Expression, and Purification

PleD mutations, D327A, R313A and R148A/R178A/R313A, were performed by using the QuickChange II Site-Directed Mutagenesis Kit (Stratagene) based on pRUN plasmids (derived from the pBR322 vector) containing the C-terminally His_6-tagged wild-type gene (Chan et al., 2004) or the R148A/R178A double mutant (Christen et al., 2006). C-terminally His_6-tagged full-length PleD and mutants were expressed in the *E. coli* BL21(DE3)pLysS strain, induced by 0.5 mM IPTG (3–4 hr, 30°C). Cells were washed twice with 20 mM Tris-HCl (pH 8.0), 500 mM NaCl buffer and were stored at −80°C. The proteins were purified by affinity chromatography with 5 ml HisTrap columns (GE Healthcare) and ~200 mM imidazole for elution. The pooled protein fractions were concentrated and further purified by size-exclusion (SEC) chromatography by using the Superdex 200 HR 26/60 column (GE Healthcare) and 20 mM Tris-HCL (pH 8.0), 100 mM NaCl as running buffer (SEC buffer). For this step, the protein concentration was kept low (5–10 mg/ml) to ensure dissociation and removal of bound c-diGMP. The protein was concentrated to 10 mg/ml, aliquoted, and stored at −20°C for further use.

Activation of PleD by BeF_3^- Modification

Activation of PleD was accomplished by supplementing the SEC buffer with $BeCl_2$, NaF, and either $MgCl_2$ or $MnCl_2$ (A buffer). Final concentrations were 200 μM for PleD, 1 mM for $BeCl_2$, 10 mM for NaF, 10 mM for $MgCl_2$, and 1 mM for $MnCl_2$. The protein was incubated for at least 30 min before experiments were conducted.

C-di-GMP

Pure samples of c-di-GMP were obtained from N. Amiot, Department of Chemistry, University of Basel. It was chemically synthesized according to procedures by Amiot et al. (2006).

Enzymatic Assays

DGC activity of wild-type and mutant PleD was analyzed by monitoring the production of pyrophosphate by using a pyrophosphatase-coupled spectrophotometric assay. Details are given elsewhere (Chan

et al., 2004). The kinetic data were fitted to numerical simulations of a scheme of noncompetitive product inhibition by using the program Berkeley Madonna.

Analytical Size-Exclusion Chromatography

Dimerization of PleD was monitored by size-exclusion chromatography (SEC) by using a Superdex 200 HR 10/30 column (GE Healthcare). SEC and A buffers were used as running buffers for nonactivated and activated protein samples, respectively. Runs were performed on an ÄKTA*purifier* (GE Healthcare) system at a flow rate of 0.7 ml/min. The concentrations of the eluted peak fractions were measured by an online refractometer (Optilab rEX, Wyatt Technology).

Isothermal Titration Calorimetry

Samples of the PleD mutant protein R313A were first diluted 15-fold either in SEC or A buffer (containing Mn^{2+} as divalent cation) and then concentrated by using a 15 ml Amicon Ultra MWCO 10 kDa (Millipore) concentrator. Protein samples and buffers were degassed (ThermoVac, MicroCal) at 2° below the temperature used in the experiments before loading into the VP-isothermal titration calorimetry (ITC) (Microcal, Northampton, MA). Details of the ITC measurement procedure and analysis of self-association have been described previously (McPhail and Cooper, 1997; Velazquez-Campoy et al., 2004). In short, 10 μl samples of nonactivated (two experiments at concentrations 929 μM and 861 μM) and activated (108 μM and 99 μM) PleD were injected into the cell filled with buffer (1.4 ml volume) at 6 min intervals. The measurements of nonactivated and activated protein were performed at 15°C and at 10°C, respectively. Both measurements of each state were fit together to obtain global ΔH and K_D values. A constant background heat, produced by the dilution of the titrant, residual differences in the buffer composition in syringe and cell, and technical effects was eliminated by allowing for a constant heat contribution (Q_{dil}) as another fit parameter upon data evaluation.

Crystallography

Crystallization of activated PleD was performed at room temperature by the hanging-drop vapor-diffusion technique. Before crystallization, c-di-GMP and Rp-GTP-α-S (BioLog) were added with final concentrations of 0.2 mM and 1 mM, respectively, to BeF_3^-/Mg^{2+}-modified PleD samples (final concentration 100 μM). A (1 μl + 1 μl) mixture of protein and well solution (0.1 M HEPES [pH 8.0], 0.73 M Na_2SO_4) gave rise to crystals of needle shape. Diffraction data were collected from a single crystal at the Swiss Light Source, Paul-Scherrer-Institute, Villigen, Switzerland, and were processed with MOSFLM/SCALA (CCP4, 1994). Orientations and positions of individual domains were determined by molecular replacement with the structure of nonactivated PleD (PDB code 1W25) by using PHASER (McCoy, 2007). The model was built by using COOT (Emsley and Cowtan, 2004) and was refined with REFMAC (CCP4, 1994). Two-fold NCS restraints were imposed.

Supplemental Data

Supplemental data include a figure of the modeled structure of the competent PleD-substrate complex, a figure of the PleD-product complex and a figure with the kinetic data of wild-type and mutant PleD and are available at http://www.structure.org/cgi/content/full/15/8/915/DC1/.

ACKNOWLEDGMENTS

Dietrich Samoray and Arnaud Baslé are greatly acknowledged for expert technical support. We thank the staff of the Swiss Light Source (SLS, PSI, Villigen, Switzerland) for assistance with data collection and N. Amiot, Department of Chemistry, University of Basel, for the gift of chemically synthesized c-di-GMP. We thank Dietrich Samoray, Dagmar Klostermeier, and Zora Markovic-Housley for critical reading of the manuscript. The work was supported by grant 3100A0-105587 of the Swiss National Science Foundation (to T.S.).

Received: January 27, 2007
Revised: June 25, 2007
Accepted: June 25, 2007
Published: August 14, 2007

REFERENCES

Aldridge, P., Paul, R., Goymer, P., Rainey, P., and Jenal, U. (2003). Role of the GGDEF regulator PleD in polar development of *Caulobacter crescentus*. Mol. Microbiol. *47*, 1695–1708.

Amikam, D., and Galperin, M.Y. (2006). PilZ domain is part of the bacterial c-di-GMP binding protein. Bioinformatics *22*, 3–6.

Amiot, N., Heintz, K., and Giese, B. (2006). New approach for the synthesis of c-di-GMP and its analogues. Synthesis *24*, 4290–4296.

Bachhawat, P., Swapna, G.V., Montelione, G.T., and Stock, A.M. (2005). Mechanism of activation for transcription factor PhoB suggested by different modes of dimerization in the inactive and active states. Structure *13*, 1353–1363.

Birck, C., Mourey, L., Gouet, P., Fabry, B., Schumacher, J., Rousseau, P., Kahn, D., and Samama, J.P. (1999). Conformational changes induced by phosphorylation of the FixJ receiver domain. Struct. Fold. Des. *7*, 1505–1515.

CCP4 (Collaborative Computational Project, Number 4) (1994). The CCP4 suite: programs for protein crystallography. Acta Crystallogr. D Biol. Crystallogr. *50*, 760–763.

Chan, C., Paul, R., Samoray, D., Amiot, N.C., Giese, B., Jenal, U., and Schirmer, T. (2004). Structural basis of activity and allosteric control of diguanylate cyclase. Proc. Natl. Acad. Sci. USA *101*, 17084–17089.

Christen, B., Christen, M., Paul, R., Schmid, F., Folcher, M., Jenoe, P., Meuwly, M., and Jenal, U. (2006). Allosteric control of cyclic di-GMP signaling. J. Biol. Chem. *281*, 32015–32024.

Christen, M., Christen, B., Allan, M.G., Folcher, M., Jeno, P., Grzesiek, S., and Jenal, U. (2007). DgrA is a member of a new family of cyclic diguanosine monophosphate receptors and controls flagellar motor function in *Caulobacter crescentus*. Proc. Natl. Acad. Sci. USA *104*, 4112–4117.

Djordjevic, S., Goudreau, P.N., Xu, Q., Stock, A.M., and West, A.H. (1998). Structural basis for methylesterase CheB regulation by a phosphorylation-activated domain. Proc. Natl. Acad. Sci. USA *95*, 1381–1386.

Doublie, S., Tabor, S., Long, A.M., Richardson, C.C., and Ellenberger, T. (1998). Crystal structure of a bacteriophage T7 DNA replication complex at 2.2 Å resolution. Nature *391*, 251–258.

Egli, M., Gessner, R.V., Williams, L.D., Quigley, G.J., van der Marel, G.A., van Boom, J.H., Rich, A., and Frederick, C.A. (1990). Atomic-resolution structure of the cellulose synthase regulator cyclic diguanylic acid. Proc. Natl. Acad. Sci. USA *87*, 3235–3239.

Emsley, P., and Cowtan, K. (2004). Coot: model-building tools for molecular graphics. Acta Crystallogr. D Biol. Crystallogr. *60*, 2126–2132.

Jenal, U., and Malone, J. (2006). Mechanisms of cyclic-di-GMP signaling in bacteria. Annu. Rev. Genet. *40*, 385–407.

Lee, S.Y., Cho, H.S., Pelton, J.G., Yan, D., Berry, E.A., and Wemmer, D.E. (2001). Crystal structure of activated CheY. Comparison with other activated receiver domains. J. Biol. Chem. *276*, 16425–16431.

Lewis, R.J., Brannigan, J.A., Muchova, K., Barak, I., and Wilkinson, A.J. (1999). Phosphorylated aspartate in the structure of a response regulator protein. J. Mol. Biol. *294*, 9–15.

Liaw, Y.C., Gao, Y.G., Robinson, H., Sheldrick, G.M., Sliedregt, L.A., van der Marel, G.A., van Boom, J.H., and Wang, A.H. (1990). Cyclic diguanylic acid behaves as a host molecule for planar intercalators. FEBS Lett. *264*, 223–227.

Malone, J.G., Williams, R., Christen, M., Jenal, U., Spiers, A.J., and Rainey, P.B. (2007). The structure-function relationship of WspR,

a *Pseudomonas fluorescens* response regulator with a GGDEF output domain. Microbiology *153*, 980–994.

Maris, A.E., Sawaya, M.R., Kaczor-Grzeskowiak, M., Jarvis, M.R., Bearson, S.M., Kopka, M.L., Schroder, I., Gunsalus, R.P., and Dickerson, R.E. (2002). Dimerization allows DNA target site recognition by the NarL response regulator. Nat. Struct. Biol. *9*, 771–778.

McCoy, A.J. (2007). Solving structures of protein complexes by molecular replacement with Phaser. Acta Crystallogr. D Biol. Crystallogr. *63*, 32–41.

McPhail, D., and Cooper, A. (1997). Thermodynamics and kinetics of dissociation of ligand-induced dimers of vancomycin antibiotics. J. Chem. Soc., Faraday Trans. *93*, 2283–2289.

Nowak, E., Panjikar, S., Konarev, P., Svergun, D.I., and Tucker, P.A. (2006). The structural basis of signal transduction for the response regulator PrrA from *Mycobacterium tuberculosis*. J. Biol. Chem. *281*, 9659–9666.

Paul, R., Weiser, S., Amiot, N.C., Chan, C., Schirmer, T., Giese, B., and Jenal, U. (2004). Cell cycle-dependent dynamic localization of a bacterial response regulator with a novel di-guanylate cyclase output domain. Genes Dev. *18*, 715–727.

Robinson, V.L., Buckler, D.R., and Stock, A.M. (2000). A tale of two components: a novel kinase and a regulatory switch. Nat. Struct. Biol. *7*, 626–633.

Robinson, V.L., Wu, T., and Stock, A.M. (2003). Structural analysis of the domain interface in DrrB, a response regulator of the OmpR/PhoB subfamily. J. Bacteriol. *185*, 4186–4194.

Ryjenkov, D.A., Tarutina, M., Moskvin, O.V., and Gomelsky, M. (2005). Cyclic diguanylate is a ubiquitous signaling molecule in bacteria: insights into biochemistry of the GGDEF protein domain. J. Bacteriol. *187*, 1792–1798.

Sinha, S.C., and Sprang, S.R. (2006). Structures, mechanism, regulation and evolution of class III nucleotidyl cyclases. Rev. Physiol. Biochem. Pharmacol. *157*, 105–140.

Steegborn, C., Litvin, T.N., Levin, L.R., Buck, J., and Wu, H. (2005). Bicarbonate activation of adenylyl cyclase via promotion of catalytic active site closure and metal recruitment. Nat. Struct. Mol. Biol. *12*, 32–37.

Steitz, T.A. (1999). DNA polymerases: structural diversity and common mechanisms. J. Biol. Chem. *274*, 17395–17398.

Stock, A.M., Robinson, V.L., and Goudreau, P.N. (2000). Two-component signal transduction. Annu. Rev. Biochem. *69*, 183–215.

Tesmer, J.J., Sunahara, R.K., Johnson, R.A., Gosselin, G., Gilman, A.G., and Sprang, S.R. (1999). Two-metal-Ion catalysis in adenylyl cyclase. Science *285*, 756–760.

Tischler, A.D., and Camilli, A. (2004). Cyclic diguanylate (c-di-GMP) regulates *Vibrio cholerae* biofilm formation. Mol. Microbiol. *53*, 857–869.

Toro-Roman, A., Mack, T.R., and Stock, A.M. (2005a). Structural analysis and solution studies of the activated regulatory domain of the response regulator ArcA: a symmetric dimer mediated by the α4-β5-α5 face. J. Mol. Biol. *349*, 11–26.

Toro-Roman, A., Wu, T., and Stock, A.M. (2005b). A common dimerization interface in bacterial response regulators KdpE and TorR. Protein Sci. *14*, 3077–3088.

Velazquez-Campoy, A., Leavitt, S.A., and Freire, E. (2004). Characterization of protein-protein interactions by isothermal titration calorimetry. Methods Mol. Biol. *261*, 35–54.

Accession Numbers

The coordinates and structure factors of activated PleD in complex with c-diGMP and Rp-GTP-α-S have been deposited in the Protein Data Bank under accession code 2v0n.